

Strong and nonmonotonic temperature dependence of Hall coefficient in superconducting $K_xFe_{2-y}Se_2$ single crystals

Xiaxin Ding, Yiming Pan, Huan Yang and Hai-Hu Wen*

Center for Superconducting Physics and Materials,

National Laboratory of Solid State Microstructures and Department of Physics, Nanjing University, Nanjing 210093, China

In-plane resistivity, magnetoresistance and Hall effect measurements have been conducted on quenched $K_xFe_{2-y}Se_2$ single crystals in order to analysis the normal-state transport properties. It is found that the Kohler's rule is well obeyed below about 80 K, but clearly violated above 80 K. Measurements of the Hall coefficient reveal a strong but non-monotonic temperature dependence with a maximum at about 80 K, in contrast to any other FeAs-based superconductors. With the two-band model analysis on the Hall coefficient, we conclude that a gap may open below 65 K. The data above 65 K are interpreted as a temperature induced crossover from a metallic state at a low temperature to an orbital-selective Mott phase at a high temperature. This is consistent with the recent data of angle resolved photoemission spectroscopy. These results call for a refined theoretical understanding, especially when the hole pockets are absent or become trivial in $K_xFe_{2-y}Se_2$ superconductors.

PACS numbers: 74.20.Rp, 74.70.Dd, 74.62.Dh, 65.40.Ba

I. INTRODUCTION

In iron-based superconductors (FeSCs), it is very important to understand the electron correlation in different bands and the orbital selective Mott transitions. As revealed by angle resolved photoemission spectroscopy (ARPES) and band structure calculations, the superconductivity and normal state of FeSCs are governed by their electronic structure involving the Fe 3d orbitals crossing the Fermi energy¹. Due to different structures and probably different methods for fabrication, the iron chalcogenide superconductors show up with different superconducting transition temperatures, for example, $T_c \approx 8$ K for $Fe_{1-x}Se$ single crystals², $T_c \approx 16$ K for $FeSe_{1-x}Te_x$ ³, $T_c \approx 32$ K for $K_xFe_{2-y}Se_2$ ^{4,5}. Furthermore, a superconducting-like gaped feature can even be found in the monolayer thin film of $FeSe/SrTiO_3$ at 65 K^{6,7}, this brings about new vitality in exploring high temperature superconductivity in the iron pnictide/chalcogenide systems.

In 2010, the discovery of the new $K_xFe_{2-y}Se_2$ superconductor has generated great excitement in the community⁸. Previously, it was proposed that the pair-scattering of electrons between the hole and electron pockets might drive the electron pairing with an S^\pm pairing symmetry^{9,10}. Nevertheless, the superconducting $K_xFe_{2-y}Se_2$ seems containing only electron pockets around the M-point, the hole pockets which appear in most FeAs based superconductors near the Γ -point are absent¹¹, which certainly leads to a challenge to explain the superconductivity by the nesting effect between the hole and electron pockets. Later on, it is found that the $K_xFe_{2-y}Se_2$ sample separates into two phases¹²⁻¹⁴ - a dominant antiferromagnetic insulating phase $K_2Fe_4Se_5$ ¹⁵⁻¹⁷, and a minority superconducting phase whose exact structure and compositions are still under debate^{13,18-20}. For the superconducting phase,

it has been gradually conceived that the main structure is still the same as the typical $BaFe_2As_2$, but both the Fe and K may be deficient, and these deficiencies may form some kind of structures. Recently, the neutron diffraction experiment indicates a potassium deficient but iron stoichiometric formula $K_xFe_2Se_2$ for the superconducting phase²¹. Therefore the study of such material is complicated by the nature of mesoscopic phase separation^{8,12,13,15,21}, and it is very challenging to explore the properties of the normal state of the superconducting phase. Recently, Yi *et al.* reported the study of ARPES on $A_xFe_{2-y}Se_2$ ($A = K, Rb$) single crystals, and proposed an orbital-selective Mott transition in the normal state²². Moreover, femtosecond pump-probe spectroscopy²³ and THz spectroscopy²⁴ studies also evidenced the Mott-transition-like behavior in the normal state. These properties are consistent with the prediction of a multiband theory assuming strong on-site Coulomb interactions²⁵. Due to the reactivity of potassium element, the sample of $K_xFe_{2-y}Se_2$ is very sensitive in air, therefore, as far as we know, the Hall effect has been seldom investigated in $K_xFe_{2-y}Se_2$. Previous preliminary measurements reveal that the Hall coefficient is negative over the whole temperature range, indicating that the system is dominated by electronic-like charge carriers^{4,5,26}, being consistent with the observation of the electron Fermi pockets in the ARPES measurements.

In this paper, we study the normal-state transport properties of quenched $K_xFe_{2-y}Se_2$ superconducting single crystals with $T_c = 32$ K through the in-plane resistivity, transverse magnetoresistance (MR) and Hall effect measurements. We find that the Kohler's rule is obeyed in the low temperature region. The Hall coefficient has a strong but non-monotonic temperature dependence below 150 K. This is in contrast with the FeAs-based systems in which the Hall coefficient shows a monotonic temperature dependence²⁷⁻²⁹. These abnormal temperature-dependent behaviors cannot be de-

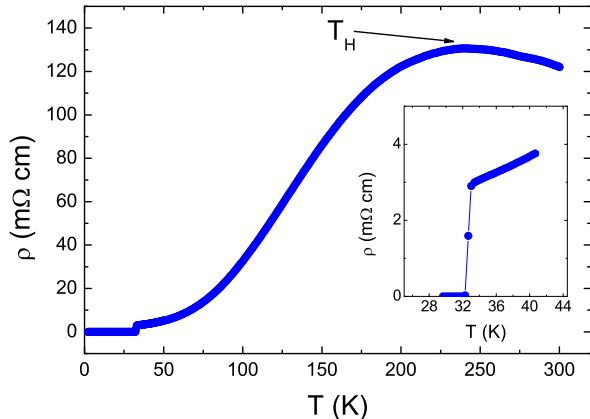


FIG. 1: (color online) Temperature dependence of in-plane resistivity measured for the quenched $K_xFe_{2-y}Se_2$ single crystal with a broad hump appearing at $T_H \sim 240$ K. A sharp superconducting transition is observed at about 32 K. An enlarged view near the superconducting transition is shown as an inset.

scribed by one single band model, suggesting the multi-band nature in $K_xFe_{2-y}Se_2$. Using a two-band model (mainly $d_{xz/yz}$ and d_{xy}) analysis, we conclude that a gap may open below 65 K, while the non-monotonic temperature dependence of the Hall coefficient could be understood as a consequence of an orbital-selective Mott transition. These results would trigger further theoretical and experimental studies of the orbital selective correlation effect in FeSCs.

II. MEASUREMENTS OF MAGNETORESISTANCE AND HALL EFFECT

The $K_xFe_{2-y}Se_2$ single crystals used for the transport measurements were fabricated by a self-flux method with a starting synthesizing composition of K:Fe:Se=0.8:2:2. The crystals are rapidly quenched in liquid nitrogen after heating to 350 °C and staying for several hours. Details of the preparation were described elsewhere²⁰. The quenching process can greatly improve the connection of the tiny superconducting networks (paths), and thus the global appearance of superconductivity is much better than the slowly cooled samples of $K_xFe_{2-y}Se_2$ ^{20,30,31}. X-ray diffraction patterns (XRD) taken on the quenched crystals show only (001) peaks with some small accompanying peaks. We think that the main diffraction (001) peaks of the XRD pattern are coming from the major part of the sample, i.e., the $K_2Fe_4Se_5$ matrix, while the small accompanying peaks are coming from the minority superconducting networks. Because there is clear evidence of phase separation in the sample, it is meaningless to claim an uniform composition through out the sample. The microanalysis using energy-dispersive-spectrum

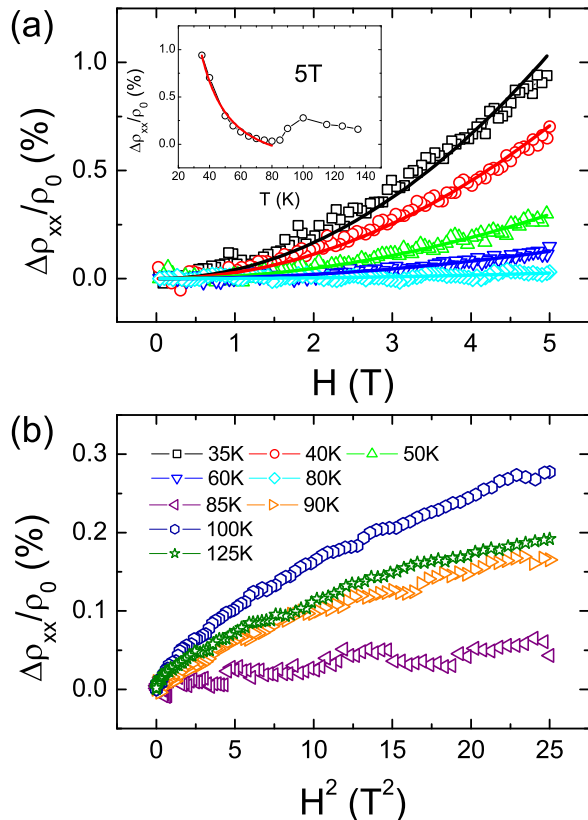


FIG. 2: Field dependence of the magnetoresistance of $K_xFe_{2-y}Se_2$. (a) The MR below 80 K. Solid lines are the fits as a function of H^2 . The inset shows temperature dependence of MR measured at a magnetic field of 5 T. A pronounced minimum occurs at 80 K. The red line is a fit to the data below 80 K as a function of T^{-2} . (b) The MR above 85 K plotted verse H^2 .

(EDS) on the samples reveals that the background has a composition close to K:Fe:Se=2:4:5. For the present quenched sample, since the minority superconducting phase (path) has very small size which is smaller than the size of the electron beam in the EDS analysis, we could not use the EDS technique directly to get valid values of compositions for the three elements²⁰. Transport measurements were carried out with the six-lead method in a Quantum Design instrument physical property measurement system (PPMS). The electric contacts were made using silver paste in a glove box filled with nitrogen atmosphere. We have worked on two samples from different batches and the results are similar to each other.

In the $K_xFe_{2-y}Se_2$ system, one concern is the phase-separation property, the superconducting and insulating phases could both contribute in transport measurements. As shown in Fig. 1, a broad hump with the peak at $T_H \sim 240$ K is observed in the normal-state, being similar to those reported previously^{4,20,30,31}. This anomaly, being

sensitive to the preparation process, could be caused by the connection in series between the metallic and the insulating phases as a result of the phase-separation picture. Hence, we mainly focus on the normal-state properties below T_H which are dominated by contributions from the metallic phase (superconducting paths below T_c). The small residual resistivity with sharp superconducting transition ($T_c = 32$ K) indicates good connectivity of the superconducting paths.

In order to get more information of the normal-state properties, further investigations are provided by the transverse MR and Hall effect measurements on the same sample. In general, for most normal metals, the MR exhibits a H^2 -dependence in the weak-field limit, and the MR normally affords a useful method to investigate the nature of electronic scattering. In Fig. 2(a), we show the field dependence of the transverse MR, $\Delta\rho_{xx}/\rho_0$, below 80 K, solid lines are fits to $\Delta\rho_{xx}/\rho_0 = aH^2$, ρ_0 is the resistivity under zero magnetic field. It is clear that the MR increases as H^2 in the sweeping magnetic field up to 5 T, signaling metallic behavior for $T \leq 80$ K, while the slight deviation at 35 K can be attributed to the superconducting fluctuations at a finite magnetic field. Besides, there is a fundamental difference in the MR between $T \leq 80$ K and $T \geq 85$ K. In the latter, as shown in Fig. 2(b), the MR seems not follow the H^2 -dependence, which indicates a transition of the electronic characteristics from one to another. The inset of Fig. 2(a) shows the temperature dependence of MR at 5 T, a clear minimum occurs at about 80 K and the MR below 80 K shows a nice fit to the T^{-2} -dependence. It is interesting to note that, the crossover at around 80 K is consistent with the measurement of the finite-frequency dielectric function by means of terahertz spectroscopy in a Rb-based sister compound³².

The Kohler's rule³³, which assumes a simple scaling function of $\Delta\rho/\rho_0 = F(H/\rho_0)$, should be satisfied for a single band metal with an isotropic Fermi surface, with ρ_0 the resistivity at a fixed temperature and zero field. For a multiband system, this rule is also applicable as long as the number of charge carriers from each band is independent on temperature and the scattering rates of different bands have the similar temperature dependence³⁴. From the first glance at the data below 60 K, as shown in Fig. 3(a), it seems that the Kohler's rule is slightly violated. Actually this slight "deviation" of Kohler's rule may not be true. The reason is that the resistivity at zero field, namely $\rho_0(T) = \rho_0(T=0) + A/\tau$ does not really reflect directly the scattering rate $1/\tau$ when the residual resistivity is sizable. In addition, as argued below, there maybe a partial gap opening below 65 K, which may give an influence of the Kohler's scaling rule. Instead of using the original scaling function $\Delta\rho/\rho_0 = F(H/\rho_0)$, we use here a more accurate form of the Kohler's scaling rule $\Delta\rho/\rho_0 = F(H\tau)$ where τ is the relaxation rate³⁵. Since the system exhibits metallic properties in the low temperature region, we could assume the relaxation rate as $\tau \propto T^{-2}$. Fig. 3(b) shows the refined Kohler's plot

of $\Delta\rho/\rho_0$ vs $(H\tau)^2 \propto (HT^{-2})^2$. One can see that the Kohler's rule is well obeyed below 80 K if we assume a general scattering rate $1/T^2$. In contrast, the Kohler's rule is drastically violated above 85 K, as shown with the enlarged view in the inset of Fig. 3(a).

We now switch our attention to the temperature dependence of Hall coefficient. In the present $K_x\text{Fe}_{2-y}\text{Se}_2$ system, Hall effect measurements may provide the message concerning the temperature dependence of the charge carrier density and mobilities of electrons in different bands of the superconducting phase. Since the insulating phase $K_2\text{Fe}_4\text{Se}_5$ has the nearest band 300 meV below the Fermi energy, they should not contribute in the Hall effect measurements below T_H . In Fig. 4(a), we show the Hall resistivity ρ_{xy} versus magnetic field up to 5 T, a linear relation between ρ_{xy} and magnetic field H has been found in wide temperature region (35 K to 150 K). From the $\rho_{xy}(H)$ data, the Hall coefficient R_H is determined through $R_H = \rho_{xy}/H$ and shown in Fig. 4(b). The negative R_H over the whole temperature region up to 150 K reveals that the conduction is dominated by electron-like charge carriers. However, the most remarkable feature in Fig. 4(b) is that the $R_H(T)$ shows a strong but non-monotonic temperature dependence. This is in sharp contrast with the FeAs-based 122 samples in which the Hall coefficient is monotonically dependent on temperature²⁷⁻²⁹. By having a closer scrutiny to the temperature dependence of Hall coefficient, two characteristic temperatures could be defined: $T_{gap} = 65$ K and $T_{mott} = 85$ K. Below 65 K, R_H decreases rapidly with a suppression towards lower temperatures. This is quite similar to that in the FeAs-based superconductors. Between 65 K and 85 K, R_H is almost temperature independent, while it decreases upon raising temperature from 85 K to 150 K. This anomalous behavior has never been reported in previous studies in $K_x\text{Fe}_{2-y}\text{Se}_2$ and suggests that something beyond the multi-band physics is very important here in determining the electric conduction.

III. DISCUSSION

According to the band structure calculations and ARPES studies, two sets of electronic orbitals near the Fermi level, namely d_{xy} and $d_{xz/yz}$ play an important role. Since the d_{xz} and d_{yz} are normally degenerate, we thus use a two band model to handle the issue. Based on the Boltzmann transport theory in the weak field limit, the equation of the Hall coefficient for two-band model could be simplified as

$$R_H = \frac{\sigma_1^2 R_{H1} + \sigma_2^2 R_{H2}}{(\sigma_1 + \sigma_2)^2} = \frac{n_1\mu_1^2 + n_2\mu_2^2}{-e(n_1\mu_1 + n_2\mu_2)^2} \quad (1)$$

where $\sigma_1 = en_1\mu_1, \sigma_2 = en_2\mu_2$ and $R_{H1} = -1/en_1, R_{H2} = -1/en_2$ are single band conductivity and Hall coefficients for the two orbitals, respectively. Based

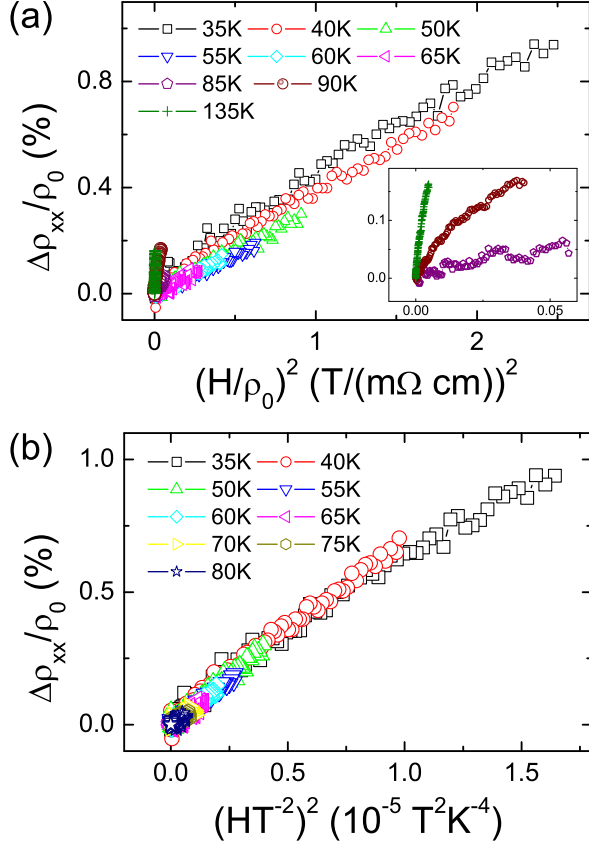


FIG. 3: (color online) (a) The scaling of Kohler's rule using $\Delta\rho/\rho_0 = F(H/\rho_0)$ at various denoted temperatures. Inset shows the Kohler's scaling of MR in low field region for selective temperatures. (b) A refined Kohler's plot below 80 K using $\Delta\rho/\rho_0 = F(H\tau)$ and assuming $1/\tau \propto T^{-2}$.

on the MR analysis, the system exhibits metallic state below 80 K and a T^{-2} temperature dependence was found in our data. Thus, the mobility of the two orbitals are expressed generally as $\mu_i = \alpha_1 T^{-2}$ ($i = 1, 2$), α_1 is a parameter related to the effective density of states. Since the Kohler's rule is well obeyed below 80 K, concerning the fact that the recent THz spectroscopy experiments on $\text{Rb}_{1-x}\text{Fe}_{2-y}\text{Se}_2$ report a gap-like suppression of optical conductance below 61 K²⁴, we thus attribute the temperature dependence of the Hall coefficient below 65 K to the temperature dependent of the charge carrier density. In this scenario we then define the carrier densities as $n_1 = n_1^0 \exp(-\Delta/k_B T)$ and $n_2 = n_2^0 \exp(-\Delta/k_B T)$ where Δ is a partial gap which opens at 65 K. The red line in Fig. 4(b) presents excellent fitting results with the two-band model. One may suggest that the temperature dependence of the Hall coefficient R_H below 65 K is related to the different temperature dependence of the scattering rate $1/\tau_i$ ($i = 1, 2$), this however cannot get support from other experiments, for example the ARPES

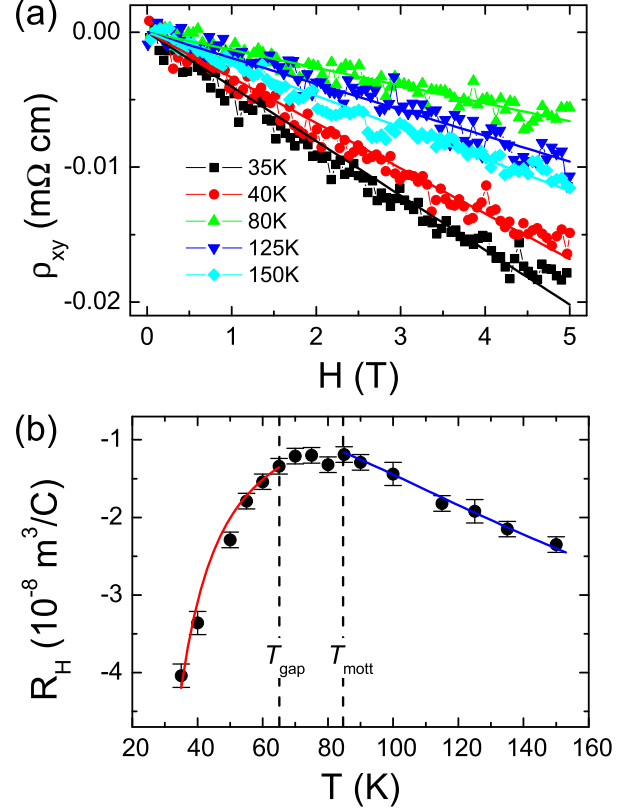


FIG. 4: (color online) (a) The transverse resistivity versus the magnetic field at different temperatures. Solid lines are linear fits. (b) Temperature dependence of Hall coefficient R_H , two characteristic temperatures could be defined: $T_{\text{gap}} = 65$ K and $T_{\text{mott}} = 85$ K. Solid lines are theoretical curves using the two-band model (see text).

and optical data.

After crossing a maximum, R_H drops with increasing temperature above 85 K, which signals the involvement of a distinct electron scattering mechanism. This turning point and the change of the temperature dependence is consistent with the results of MR analysis. Recently, an orbital-selective Mott transition was observed by ARPES at about 90 K in the superconducting phase of $\text{K}_x\text{Fe}_{2-y}\text{Se}_2$, where the spectral weight near Fermi surface for the d_{xy} orbital diminishes while the other orbitals $d_{xz/yz}$ remain metallic²². Moreover, investigations using pump-probe spectroscopy²³ and THz spectroscopy²⁴ also evidenced the Mott-transition related behavior in the normal state. This scenario could give a reasonable explanation to our data here. Since the $d_{xz/yz}$ orbital remains metallic, we still express the mobility of $d_{xz/yz}$ orbital as $\mu_1 = \alpha_1 T^{-2}$ and the carrier density as a constant n_1^0 . Meanwhile, we consider that the d_{xy} band goes into the Mott phase with raising temperature. As it is well known, the Mott insulating behav-

ior has been experimentally identified and theoretically explained in terms of the band narrowing effect associated with the electron-electron correlation. Therefore, the mobility of d_{xy} orbital could be interpolated with the formula $\mu_2 = \alpha_2 T^{-\beta} / (1 + \gamma T)$, where $1/(1 + \gamma T)$ is the modification term associated with the Mott transition. To approach a solution, we may set the carrier density of the d_{xy} orbital as a constant n'_2 for simplicity. Thus, the expression of the Hall coefficient with the orbital-selective Mott phase is written as

$$R_H = \frac{n_1^0 (\alpha T^{-2})^2 + n'_2 \left(\frac{T^{-\beta}}{1+\gamma T}\right)^2}{-e(n_1^0 \alpha T^{-2} + n'_2 \left(\frac{T^{-\beta}}{1+\gamma T}\right)^2)} \quad (2)$$

where $\alpha = \alpha_1/\alpha_2$ is the relative ratio of the mobility coefficient of the two orbitals. In Fig. 4(b), the blue solid line above 85 K shows the theoretical fitting result. Consequently, we acquire the parameters as $\Delta = 7.7$ meV, $n_1^0 = 9 \times 10^{26} \text{ m}^{-3}$, $n_2^0 = 9 \times 10^{26} \text{ m}^{-3}$, $n'_2 = 1.1 \times 10^{26} \text{ m}^{-3}$, $\alpha = 500$, $\beta = 0.2$ and $\gamma = 0.001 \text{ K}^{-1}$. The plateau of the Hall coefficient R_H between 65 K and 85 K may be viewed as the crossover of the two different regions.

We note that the appearance of a gap with the value of $\Delta = 7.7$ meV below 65 K could be compared to the observation of high-temperature superconductivity at 65 K in single-layer FeSe films^{6,7}. We also can't rule out the possibility of a pseudogap opening or other explanations for this gap-like suppression of R_H below 65 K. The decrease of R_H for increasing temperature starting from 85 K can get a strong support from the scenario of

the orbital-selective Mott transition in this system. The explanation based on the orbital selective Mott transition should call for further theoretical and experimental efforts.

IV. CONCLUSION

In summary, magnetoresistance and Hall coefficient R_H have been measured in superconducting $\text{K}_x\text{Fe}_{2-y}\text{Se}_2$ single crystals. The Kohler's rule is well obeyed below 80 K by assuming a general scattering rate $1/\tau \propto T^2$. We have observed a strong and non-monotonic temperature dependence of the Hall coefficient in the normal state. Using a two-band model analysis and combining with the published data of the time domain optical conductivity measurements, we conclude that a gap may open below 65 K, while the data above 85 K could be understood as a consequence of an orbital-selective Mott transition of the d_{xy} band.

Acknowledgments

We appreciate the useful discussions with Qimiao Si and the help of Baigen Wang. This work is supported by the NSF of China (11034011/A0402), the Ministry of Science and Technology of China (973 projects: 2011CBA00102 and 2012CB821403) and PAPD.

* hhwen@nju.edu.cn

* Electronic address: hhwen@nju.edu.cn

¹ P. Hirschfeld, M. Korshunov, and I. Mazin, Reports on Progress in Physics **74**, 124508 (2011).
² P. F.-C. Hsu, J.-Y. Luo, K.-W. Yeh, T.-K. Chen, T.-W. Huang, P. M. Wu, Y.-C. Lee, Y.-L. Huang, Y.-Y. Chu, D.-C. Yan, et al., Proceedings of the National Academy of Sciences **105**, 14262 (2008).
³ K.-W. Yeh, T.-W. Huang, Y.-L. Huang, T.-K. Chen, F.-C. Hsu, P. M. Wu, Y.-C. Lee, Y.-Y. Chu, C.-L. Chen, J.-Y. Luo, et al., EPL **84**, 37002 (2008).
⁴ J. Guo, S. Jin, G. Wang, S. Wang, K. Zhu, T. Zhou, M. He, and X. Chen, Phys. Rev. B **82**, 180520 (2010).
⁵ M.-H. Fang, H.-D. Wang, C.-H. Dong, Z.-J. Li, C.-M. Feng, J. Chen, and H. Yuan, EPL **94**, 27009 (2011).
⁶ D. Liu, W. Zhang, D. Mou, J. He, Y.-B. Ou, Q.-Y. Wang, Z. Li, L. Wang, L. Zhao, S. He, et al., Nature Communications **3**, 931 (2012).
⁷ S. He, J. He, W. Zhang, L. Zhao, D. Liu, X. Liu, D. Mou, Y.-B. Ou, Q.-Y. Wang, Z. Li, et al., Nature Materials **12**, 605 (2013).
⁸ H.-H. Wen, Reports on Progress in Physics **75**, 112501 (2012).
⁹ I. Mazin, D. J. Singh, M. Johannes, and M.-H. Du, Phys. Rev. Lett. **101**, 057003 (2008).
¹⁰ K. Kuroki, S. Onari, R. Arita, H. Usui, Y. Tanaka, H. Kon-

tani, and H. Aoki, Phys. Rev. Lett. **101**, 087004 (2008).
¹¹ I. Shein and A. Ivanovskii, Phys. Lett. A **375**, 1028 (2011).
¹² B. Shen, B. Zeng, G. Chen, J. He, D. Wang, H. Yang, and H. Wen, EPL **96**, 37010 (2011).
¹³ W. Li, H. Ding, P. Deng, K. Chang, C. Song, K. He, L. Wang, X. Ma, J.-P. Hu, X. Chen, et al., Nature Physics **8**, 126 (2012).
¹⁴ Y. Zhang, L. Yang, M. Xu, Z. Ye, F. Chen, C. He, H. Xu, J. Jiang, B. Xie, J. Ying, et al., Nature Materials **10**, 273 (2011).
¹⁵ D. Ryan, W. Rowan-Weetaluktuk, J. Cadogan, R. Hu, W. Straszheim, S. Budko, and P. Canfield, Phys. Rev. B **83**, 104526 (2011).
¹⁶ W. Bao, Q.-Z. Huang, G.-F. Chen, M. A. Green, D.-M. Wang, J.-B. He, and Y.-M. Qiu, Chin. Phys. Lett. **28**, 086104 (2011).
¹⁷ F. Ye, S. Chi, W. Bao, X. Wang, J. Ying, X. Chen, H. Wang, C. Dong, and M. Fang, Phys. Rev. Lett. **107**, 137003 (2011).
¹⁸ W. Li, H. Ding, Z. Li, P. Deng, K. Chang, K. He, S. Ji, L. Wang, X. Ma, J.-P. Hu, et al., Phys. Rev. Lett. **109**, 057003 (2012).
¹⁹ Y. Texier, J. Deisenhofer, V. Tsurkan, A. Loidl, D. Inosov, G. Friemel, and J. Bobroff, Phys. Rev. Lett. **108**, 237002 (2012).

- ²⁰ X. Ding, D. Fang, Z. Wang, H. Yang, J. Liu, Q. Deng, G. Ma, C. Meng, Y. Hu, and H.-H. Wen, *Nature Communications* **4**, 1897 (2013).
- ²¹ S. V. Carr, D. Louca, J. Siewenie, Q. Huang, A. Wang, X. Chen, and P. Dai, *Phys. Rev. B* **89**, 134509 (2014).
- ²² M. Yi, D. Lu, R. Yu, S. Riggs, J.-H. Chu, B. Lv, Z. Liu, M. Lu, Y.-T. Cui, M. Hashimoto, et al., *Phys. Rev. Lett.* **110**, 067003 (2013).
- ²³ W. Li, C. Zhang, S. Liu, X. Ding, X. Wu, X. Wang, H.-H. Wen, and M. Xiao, *Phys. Rev. B* **89**, 134515 (2014).
- ²⁴ Z. Wang, M. Schmidt, J. Fischer, V. Tsurkan, M. Greger, D. Vollhardt, A. Loidl, and J. Deisenhofer, *Nature Communications* **5** (2014).
- ²⁵ R. Yu and Q. Si, *Phys. Rev. Lett.* **110**, 146402 (2013).
- ²⁶ X. Luo, X. Wang, J. Ying, Y. Yan, Z. Li, M. Zhang, A. Wang, P. Cheng, Z. Xiang, G. Ye, et al., *New J. Phys.* **13**, 053011 (2011).
- ²⁷ P. Cheng, H. Yang, Y. Jia, L. Fang, X. Zhu, G. Mu, and H.-H. Wen, *Phys. Rev. B* **78**, 134508 (2008).
- ²⁸ H. Luo, P. Cheng, Z. Wang, H. Yang, Y. Jia, L. Fang, C. Ren, L. Shan, and H.-H. Wen, *Physica C: Superconductivity* **469**, 477 (2009).
- ²⁹ L. Fang, H. Luo, P. Cheng, Z. Wang, Y. Jia, G. Mu, B. Shen, I. Mazin, L. Shan, C. Ren, et al., *Phys. Rev. B* **80**, 140508 (2009).
- ³⁰ F. Han, H. Yang, B. Shen, Z.-Y. Wang, C.-H. Li, and H.-H. Wen, *Philosophical Magazine* **92**, 2553 (2012).
- ³¹ Y. Liu, Q. Xing, K. W. Dennis, R. W. McCallum, and T. A. Lograsso, *Phys. Rev. B* **86**, 144507 (2012).
- ³² A. Charnukha, J. Deisenhofer, D. Pröpper, M. Schmidt, Z. Wang, Y. Goncharov, A. N. Yaresko, V. Tsurkan, B. Keimer, A. Loidl, and A. V. Boris, *Phys. Rev. B* **85**, 100504 (R)(2012).
- ³³ A. B. Pippard, *Magnetoresistance in metals*, 2 (Cambridge University Press, 1989).
- ³⁴ M. Chan, M. Veit, C. Dorow, Y. Ge, Y. Li, W. Tabis, Y. Tang, X. Zhao, N. Barišić, and M. Greven, *arXiv:1402.4472* (2014).
- ³⁵ N. Luo, and G. H. Miley, *Physica C* **371**, 259 (2002).